

# Numerical Simulation of the Flow Field around a Gravity Platform

**Xin Wang**

*College of engineering in Ocean University of China, Laoshan District Songling ROAD NO.238, Qing Dao, China, Doctor*  
*College of architectural engineering in Qing Dao Agricultural University, Chengyang District Changcheng ROAD NO.700, Qing Dao, China, lecturer; e-mail: betty\_wx@126.com*

**Yinbang Wang**

*College of engineering in Ocean University of China, Laoshan District Songling ROAD NO.238, Qing Dao, China. Prof. Dr tutor; e-mail: wangyb@ouc.edu.cn*

**Nan Liu**

*College of engineering in Ocean University of China, Laoshan District Songling ROAD NO.238, Qing Dao, China, Doctor; e-mail: liunan.8407@163.com*

**Yingjie Yang**

*College of engineering in Ocean University of China, Laoshan District Songling ROAD No. 238, Qing Dao, China, Master; e-mail: yangyingjie100@163.com.*

## ABSTRACT

In order to predict the local scour around the gravity platform, the paper simulated the flow field around the platform in two dimensional space with large eddy numerical simulation method and SIMPLEC pressure correction algorithm, which based on the finite volume method. Through the average flow field characteristics and integral parameters got, the basic characteristics of the wake structure could be understood.

**KEYWORDS:** gravity platform; LES; SIMPLEC

## INTRODUCTION

A new type of platform, called gravity platform was used to exploit the marginal oilfield, where the reserves is small and production period is short. The platform is generally built by steel or reinforced concrete, and fixed in the bottom of the sea by gravity itself. Like other forms of platform, the presence of gravity platform will change its surrounding flow conditions, and cause local scour of the seabed, then threaten the stability of the platform. Predecessors had already done a lot of work about the flow and local scouring near the pile, but mostly through experiments to finish. For example, in the earliest time, Roshoko [1] found that there were three

different wake flow states related to the Reynolds number existing in the flow around pile. Through the flow field display technology, Taneda[2-3] observed that the cylindrical wake flow evolved into secondary vortex with lower frequency than primary vortex when the downstream distance increasing, etc.

With the rapid development of numerical simulation technology in recent years, computational fluid dynamics (CFD) have stood more and more outstanding position when simulating the flow around a body and scouring<sup>[4]</sup>. Such as large eddy simulation (LES) made certain progress when used in the local flow simulation, and three dimensional k- $\epsilon$  model is suitable for the local scour simulation combined with sediment model.

Mendoza & Cabrera (1993) simulated the flow field around the vertical cylinder and the bed shear stress through solving three dimensional RANS and standard k- $\epsilon$  turbulence model, then found that the results were more far away from the experimental data, which mainly because that the standard k- $\epsilon$  model is not suitable to solve three-dimensional cylindrical flow<sup>[5]</sup>. Breuer<sup>[6]</sup> simulated the flow with  $Re = 140000$  around cylinder through LES, and the results were full coincided with experiment results. After simulated the flow field around the cylindrical pier with standard k- $\epsilon$  turbulent model and contrasted with the actual measurement in detail, Istiarto (2001) found that the velocity simulated is coincide with the measured values relatively and the predicted turbulent kinetic energy is smaller<sup>[7]</sup>. Ushijima simulated the three dimensional flow field accurately under the circumstances of dynamic boundary conditions in the body-fitted coordinates<sup>[8]</sup>. The paper simulated 2D flow field around the gravity platform with LES.

## THE PHYSICAL MODEL OF PLATFORM

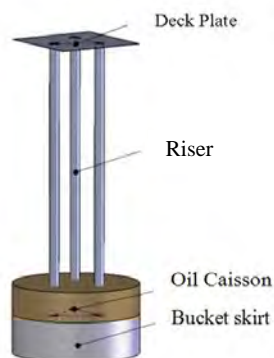


**Figure 1:** Design diagram of platform      **Figure 2:** Physical model of platform

The gravity platform, which contained deck plate, riser, bucket skirt and subsidiary facility (see Figure 1), studied in the article is fit for shallow sea of 25 meters depth. Deck plate is 9 meters higher than water surface. The size of platform is designed as follows:

Deck is a square with a side 12 meters, thickness is 15 millimeters. For riser, outer diameter is 1.2 meters, the height is 34 meters, and wall thickness is 24 millimeters. Three rises constitute

an equilateral triangle with 6 meters length of a side. One end is fixed with deck plate, the other end throughout the oil caisson and is fixed on the surfaces of the top of the bottom.

Oil caisson: inside diameter is 16 meters, the height is 3.3 meters, the thickness of the two floors is 40 centimeters the same as wall thickness.

Bucket skirt: Outside diameter is 16.8 meters which matches with oil caisson, 5meters height and 12 millimeters thick.

Physical model (see Figure 2) presented was proportional reduced with 1:25 according to actual structure, and the gravity platform was simplified into a cylinder in the paper when simulating.

## NUMERICAL SIMULATION

### Method and controlling equations

Fluent is one of the most comprehensive and extensive application computational fluid dynamics analysis software, whose simulation methods mainly include large eddy simulation, statistical average method and Reynolds average method. LES adopted in this paper decomposed the instantaneous turbulence motion through the filter method into large scales and small scales. The large scales' motion can be got by solving N-S equation directly, and the effect made by the small one can be simulated through the Subgrid-Scale model. So each random instantaneous variable can be written as

$$\phi = \bar{\phi} + \phi'$$

where  $\bar{\phi}$  is solvable large scale variable,  $\phi'$  is small one, also to be called SGS component of  $\phi$

$$\text{After filtering, } \bar{\phi} \text{ can be written as } \bar{\phi} = \int_D \phi G(x, x') dx'$$

where  $D$  is the flow field,  $x'$  is the space coordinates in  $D$ ,  $x$  is the coordinate of  $\bar{\phi}$  after

filtering, the filter function  $G(x, x')$  is the average of variable in a control volume according to

the finite volume method. Then the instantaneous continuity equation and Navier-Stokes

equation can be written as:

$$\frac{\partial \rho}{\partial t} + \frac{\partial}{\partial x_i} (\rho \bar{u}_i) = 0$$

$$\frac{\partial}{\partial t}(\rho \bar{u}_i) + \frac{\partial}{\partial x_j}(\rho \bar{u}_i \bar{u}_j) = -\frac{\partial \bar{p}}{\partial x_i} + \frac{\partial}{\partial x_j}(\mu \frac{\partial \bar{u}_i}{\partial x_j}) - \frac{\partial \tau_{ij}}{\partial x_j}$$

where the variables with overline were filtered already,  $\tau_{ij}$  is subgrid-scale stresses, short for SGS stresses, which embodies the effects made by the small scale eddies on the motion equations solved:

$$\tau_{ij} = \overline{\rho u_i u_j} - \rho \bar{u}_i \bar{u}_j$$

The SGS stress was generated by nonlinear convection item when filtering, it cannot be obtained directly by solving differential equations, so must be modeled. Because most SGS Reynolds stress model is based on the eddy viscosity hypothesis, it was thought that they are proportional to the strain rate on solvable scales. In this paper, SGS was modeled based on the Smagorinsky eddy viscosity model, where the deviator part of SGS can be expressed as

$$\tau_{ij} = -2\mu_t \bar{S}_{ij}$$

where  $\bar{S}_{ij}$  is the deformation rate tensor after filtered, and here the turbulent viscosity can be

written as  $\mu_t = (C_s \Delta)^2 |\bar{S}|$

$$\bar{S}_{ij} = \frac{1}{2} \left( \frac{\partial \bar{u}_i}{\partial x_j} + \frac{\partial \bar{u}_j}{\partial x_i} \right) \quad |\bar{S}| = \sqrt{2 \bar{S}_{ij} \bar{S}_{ij}} \quad \Delta = (\Delta_x \Delta_y \Delta_z)^{1/3}$$

where  $C_s$  is a stress constant ranged from 0.1 to 0.23, and the smaller values were adopted in order to reduce the diffusion effect made by the SGS.  $\Delta$ , the spatial filtering scale, is related to the width of the grid, and  $\Delta_i$  is the mesh size in the  $i$  direction.

## Computational domain and boundary conditions

According to the model parameters and computer calculation ability, the cylinder diameter designed as  $D = 0.084\text{m}$ , computational domain is a square with  $25D \times 15D$ , according to Sarker<sup>[9]</sup>, the downstream is unaffected if the distance away from the cylinder is more than  $12D$ , so in the paper, the cylinder will be placed  $7.5D$  away from the import.

The initial conditions and boundary conditions must be reasonable defined in order to solve flow equations more accurately, in this paper, the conditions defined as follows:

Inlet: velocity-inlet, uniform flow

Far field: Outflow

Cylinder and sea bed: free-slip boundary condition, namely  $u_n = 0$

Two sides and top surface: symmetrical boundary

Unsteady viscous fluid: reference pressure set as 1 atm.

## Meshing and solving

Based on Gambit, the flow field is divided into 9 regions (see Figure 3), and meshed intensively close to the cylinder for the flow near the cylinder wall and the wake flow near the separation point is very complicated. In order to guarantee the mesh size calculated by LES,  $y^+$  near the wall is set to be 1. Then the square near the cylinder is meshed to 4 parts according to the diagonal, and refining grid along the radius direction (see Figure 4). The whole field is meshed by structured grid and different mesh size is adopted in different regions.

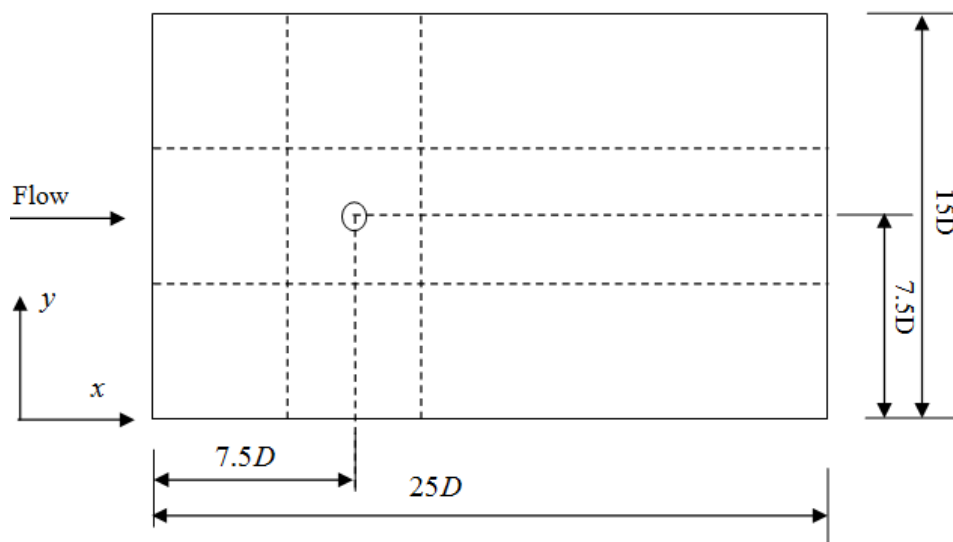


**Figure 3:** Computational domain

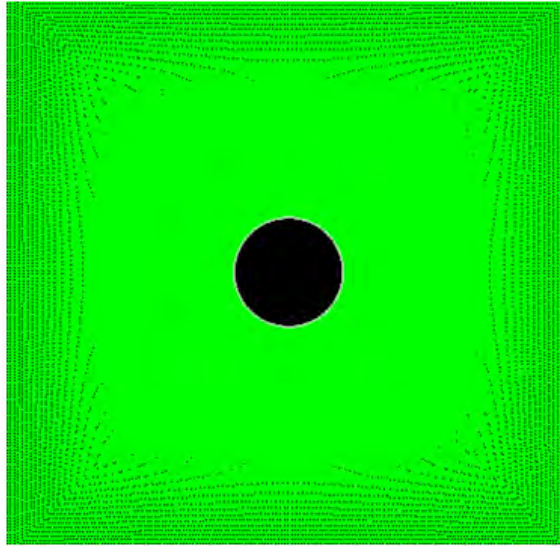


**Figure 4:** Grid near the cylinder

Dispersing the equations in collocated grids, and dispersing time with second order full implicit, time step set as  $\Delta t = 0.0005s$ . Based on finite volume method, the semi-implicit method for pressure-linked equations consistent is adopted, and the momentum equations dispersed by bounded central differencing method, pressure interpolated in second order.

## ANALYSIS OF THE RESULTS

### Characteristic Parameters

#### *1. Steady pressure coefficient*

Transient pressure can be expressed as the sum of static pressure and pulse pressure. Figure 5 gave the steady pressure coefficient's distribution along the cylindrical surface. It is a symmetrical distribution, the largest one appeared when face to the flow, and with the recovery of flow velocity, steady pressure coefficient decreased, and to the minimum when the circumferential angle at  $75^\circ$ . Subsequently pressure coefficient have rebounded, and forming a uniform pressure distribution in the cylindrical back backflow zone.

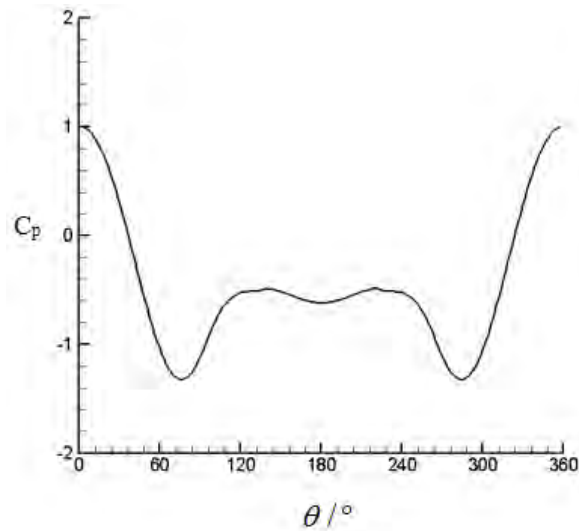


**Figure 5:** Distribution of  $C_p$

## 2. Lift coefficient and Drag coefficient

Lift coefficient and Drag coefficient were important characteristic parameters to describe the force around the cylinder made by the flow. The formula can be written as follows:

$$C_l = \frac{F_l}{\frac{1}{2}\rho u_0^2 A} \quad C_d = \frac{F_d}{\frac{1}{2}\rho u_0^2 A}$$

where  $F_l$  is the lift force vertical to the flow;  $F_d$  is the drag force in the direction of flow,  $A$  is the projection area of cylinder in the direction of calculation.

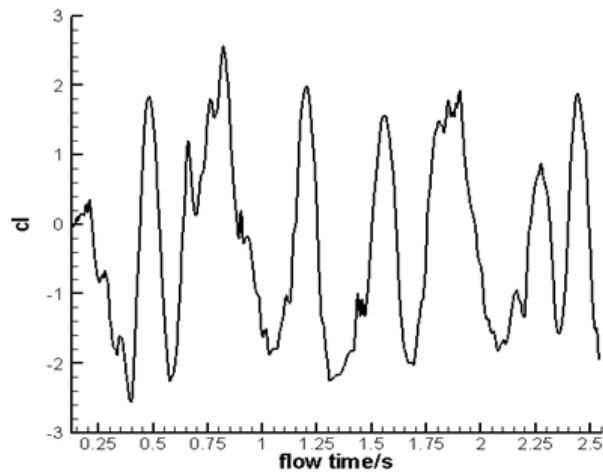


**Figure 6:** Variation of lift coefficient with time

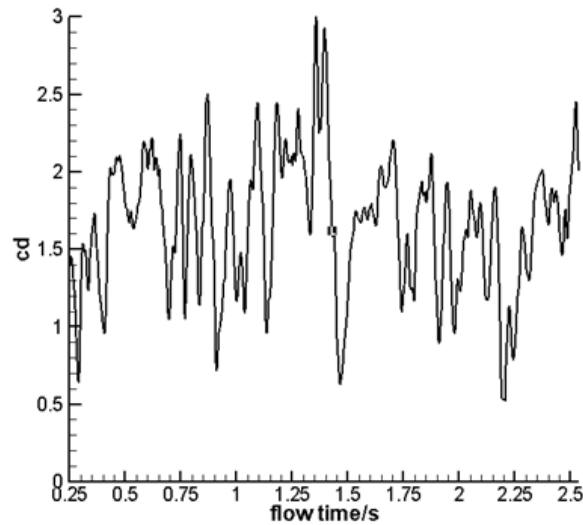


**Figure 7:** Variation of drag coefficient with time

From Figure 6 and Figure 7, we can get that the lift and drag coefficient fluctuation frequency increased, the cycle became regulate incompletely, and the amplitude changed random.

### 3. $S_{tr}$ Number

$S_{tr}$  is a characteristic parameter to describe the steadiness of vortex shedding, and also reflect the unsteady characteristics of the flow. It can be defined as

$$S_{tr} = \frac{f_d}{u_0}$$

where  $u_0$  is the velocity of flow,  $f$  is the vortex shedding frequency.

Although different from the power spectrum density of low Reynolds number, it is not unimodal, the power spectrum density of lift coefficient still have a obvious peak value (see Figure 8), which corresponding to the vortex distribution frequency, and this can be used to calculate the corresponding strouhal number.

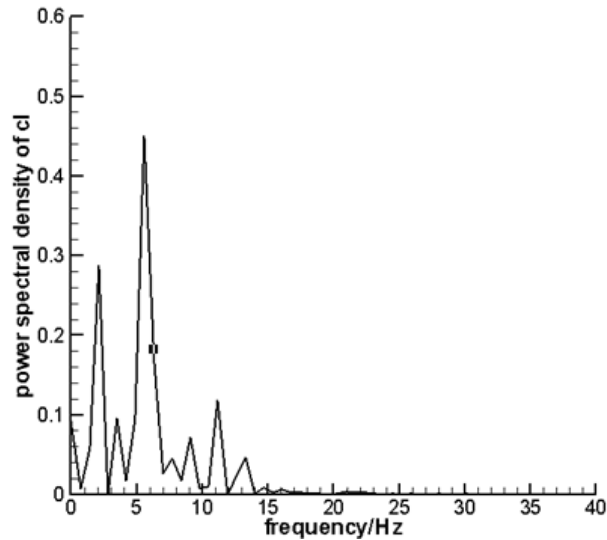


**Figure 8:** Power spectrum density of lift coefficient

## CONCLUSION

(1) Due to the resistance of the platform to the flow, water increased near the upstream of platform, and to the highest when arrived at the platform, on the other hand, water two sides concentration, the kinetic energy increased, and the water drop down.

(2) The boundary layer of the cylinder in critical region was laminar, but the vortex street behind has completely into turbulence, and issued vortex according to certain frequency.

(3) Along with the flow, large scale vortex itself became unstable, and gradually broken into small scale vortex, the energy was sent into small scale vortex. Small scale vortex ruptured further, became smaller scale vortex, this process was continuous repeated.

(4) To provide more detailed reference on scouring, 3d simulation will be done in order to get more accurate flow field distribution.

## ACKNOWLEDGEMENT

This work was financially supported by the National High Technology Research and Development Program (2007AA09Z317), Innovation Program of Ministry of Science and Technology of the People's Republic of China.

## REFERENCES

- [1] Roshoko, A. On the development of turbulent wakes from vortex streets. NACA Rep. 1954, pp. 1191.
- [2] Taneda, S. Downstream development of the wakes behind cylinder. J. Phys. Soc. Japan. Vol.14, 1959, pp. 843-848
- [3] Taneda, S. Experimental investigation of the wakes behind cylinders and Plates at low Reynolds numbers. Journal of Physical Society of Japan, Vol.11, No.3, 1956, pp. 302-307.
- [4] Fujun Wang, Analysis of computational fluid dynamics, Beijing: Tsinghua University, 2004. (In Chinese)
- [5] Mendoza-Cabrales, C. Computation of flow past a pier mounted on a flat plate. Proc. ASCE Water Resource Engineering Conf., San Francisco, 1993, pp. 899-904.
- [6] Breuer M.A challenging test case for large eddy simulation: high Reynolds number circular cylinder flow[J]. International Journal of Heat and Fluid Flow, Vol.21, No.5, 2000, pp. 648-654.
- [7] Istiarto I. Flow around a cylinder in a scoured bed. [D]. Lausanne, EPFL, 2001.
- [8] Ushijima S. Arbitrary Lagrangian-Eulerian numerical prediction for local scour caused by turbulent flows. Journal of Computational Physics, Vol.125, 1996, pp. 71-82.
- [9] Md. Akhtaruzzaman Sarker, Flow measurement around scoured bridge piers using Acoustic-Doppler Velocimeter (ADV), Vol.9, No. 4, December 1998, pp. 217-227.
- [10] Li, Z. B. (1999) Ocean Engineering and Structures [M]. Harbin: Harbin Engineering University Press, pp. 1-11 (In Chinese).
- [11] He, S. H., and Hong, X. F. (2003) Design and research of Fixed Offshore Platforms [M]. Beijing: China Petrochemical Press, pp. 14-50 (In Chinese).

